COBEM 2021 26th International Congress of Mechanical Engineering
November 22-26, 2021, Virtual Congress, Brazil

COB-2021-1388
HEMODYNAMICS ALTERATIONS INDUCED BY CENTRAL VENOUS CATHETER IN VASCULAR ACCESS FOR HEMODIALYSIS

Saulo de Freitas Gonçalves
Matheus Carvalho Barbosa Costa
Programa de Pós Graduação em Engenharia Mecânica da UFMG - Universidade Federal de Minas Gerais, Avenida Antônio Carlos, 6627, Belo Horizonte, Minas Gerais, Brazil
saulodfg@gmail.com
mt94_carvalho@hotmail.com

Mário Luis Ferreira da Silva
Programa de Pós Graduação em Engenharia Mecânica da UFMG - Universidade Federal de Minas Gerais, Avenida Antônio Carlos, 6627, Belo Horizonte, Minas Gerais, Brazil
marioluisfs@gmail.com

Thabata Coaglio Lucas
Universidade Federal dos Vales do Jequitinhonha e Mucuri, Rodovia MGT 367- km 583, 5000, Diamantina, Minas Gerais, Brasil.
thabataclugas@gmail.com

Rudolf Huebner
Programa de Pós Graduação em Engenharia Mecânica da UFMG - Universidade Federal de Minas Gerais, Avenida Antônio Carlos, 6627, Belo Horizonte, Minas Gerais, Brazil
rudolf@demec.ufmg.br

Abstract. *There is a tendency, in worldwide scenario, of increasing the number of patients on dialysis, as well as the prevalence rates in renal replacement therapy and central venous catheter use. The major cause of central venous catheters non-functionality is associated with thrombus formation. The alteration of physical properties in the flow field, induced by the presence of the catheter, may lead to a non-physiological condition of shear stress, strain rate and exposure time, which can be unfavorable in thrombogenic terms. The knowledge of how those physical properties are altered by the presence of the catheter is of fundamental importance for the optimization in the design of those devices. The present study aims to develop a numerical model to compare and analyze the hemodynamic environment in central venous access for hemodialysis, considering the presence and absence of central venous catheter. The simulations were performed in transient regime, covering two complete physiological cardiac cycles of 0.8 s. The geometry of central veins was obtained by computed tomography images of a healthy, 74-year-old male patient. A central venous catheter model similar to the clinical device MedCOMP/HEMO-CATH (Harleysville, PA, USA) was used. The K-w SST turbulence model was used to characterize turbulence. Blood was considered both as Newtonian fluid, and non-Newtonian, modeled by the Carreau-Yasuda equations. It was observed that the catheter was responsible for increasing the values of strain rate, shear stress, as well as generating regions of recirculation, stagnation, and separation of the flow field. The comparison of the percentage increase in shear stress and maximum exposure time along the streamlines, with and without catheter, reinforces the hypothesis that the exposure time may be more significant for the thrombus formation in the region than the shear stress.*

Keywords: *Hemodialysis, Central Venous Catheter, Thrombus Formation, Blood Flow, Computational Fluid Dynamics.*

1. INTRODUCTION

There is a tendency in increasing the number of patients on dialysis as well as the prevalence rates in renal replacement therapy in the worldwide scenario. It is estimated that, in 2010, there were about 2 million dialysis patients in the world and this number is expected to double by 2030 (Chan *et al.*, 2019).

In Brazil, hemodialysis remains the predominant renal clearance method adopted, currently, in about 92% of patients with end-stage renal disease, which corresponds to an increase of 3% in relation to 2009 (Neves *et al.*, 2020). Despite of arteriovenous fistulas and arteriovenous grafts has been considered the preferred form of vascular access for hemodialysis, there was an increase in the number of patients using central venous catheter (CVC), from 6% to 14% between 2013 and 2018 (Neves *et al.*, 2020).

About 50% of CVC's non-functionality is associated with the thrombus formation (Peng *et al.*, 2017; Male *et al.*, 2015). Thrombus formation process depends on the physical factors of the flow field, such as turbulence, regions of recirculation and stagnation, shear stress and particle exposure time to these shear stresses. These factors enhance the advective transport of platelets, plasma proteins and coagulation factors contained in the blood, which can favor platelet aggregation (Bream, 2016; Breg *et al.*,2018). In this context, a rational criterion for the optimization of the clinical hemodialysis procedure, and the improvement of CVC's designs, can only be performed through adequate knowledge of how the presence of the CVC can change the hemodynamic environment in the central venous access for hemodialysis.

The modification of the hemodynamic environment induced by the CVC presence, may lead to higher shear stress, strain rate, turbulence intensity and blood particles exposure time. However, the exact way and magnitude that these variables are altered, or combined, by the presence of the CVC, as well as it's impacts on the thrombus formation in the region is not well known.

Aiming to contribute to a better elucidation of these factors, this study aims to develop a numerical model, based on computational fluid dynamics, to analyze and compare the hemodynamic environment in the humans central veins of a healthy male patient (74 years old), considering the presence and absence of the catheter. The alterations in shear stress, strain rate, as well as in the global pattern of the flow field were compared and discussed considering the presence and absence of the CVC.

2. MATERIALS AND METHOODS

Ansys Fluent 19.2 software was used for numerical discretization of the continuity, momentum, and turbulence models transient equations. The blood flow was considered incompressible and modeled booth as Newtonian and non-Newtonian (Carreau-Yasuda model was employed).

2.1 Geometry

The geometry of internal jugulars vein and superior vena cava was obtained from handling computed tomography (CT) images of a male healthy patient of 74 years old. In the *InVersalius3®*, a medical image processing software, it was imported the DICOM (Digital Imaging and Communications in Medicine) files. The data files were processed in order to acquire only the region of interest. Figure 1a illustrates this procedure, with the region of interest highlighted in green. The undesirable parts, such as bone, tissue surface, among others, were removed.

Cleaning, smoothing and removal of surface imperfections to improve the surface quality were carried out in Autodesk *Meshmixer®* software. Figure 1b shows the geometry resulted of this process.

In order to facilitate manufacturing the experimental model and aiming to improve optical access for future studies, the excess of curvature of the geometry was removed. Basically, the geometry was edited in *ANSYS SpaceClaim*, to become symmetrical in relation to a central plane (XZ plane, as shown in Figure 1c).

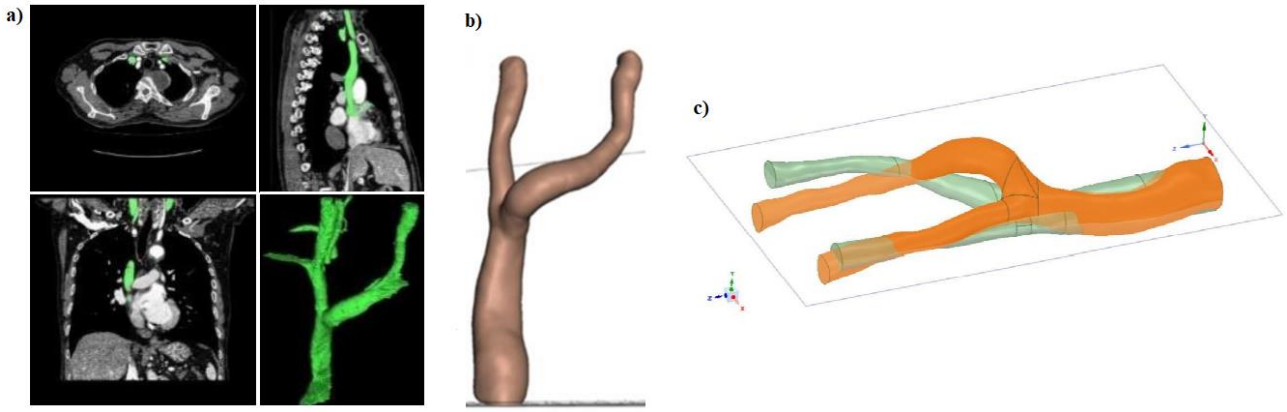

Figure 1. Geometric model of the central veins. Images cleaning and edition in *InVesalius3®*. (a) Generation and improvement of the surface quality in *Meshmixer®* (b) Geometry edition in *ANSYS SpaceClaim* (c).

In addition, *SolidWorks (SolidWorks, Inc., Concord, MA, USA)* software was used to develop a CVC geometry similar to clinical model *MedCOMP/HEMO-CATH (Harleysville, PA, USA)*. Figure 2a shows the geometrical model developed for the CVC. Figure 2b shows the geometrical model of the vein with the CVC inserted. Figure 2c shows the geometrical model of the vein without the CVC inserted.

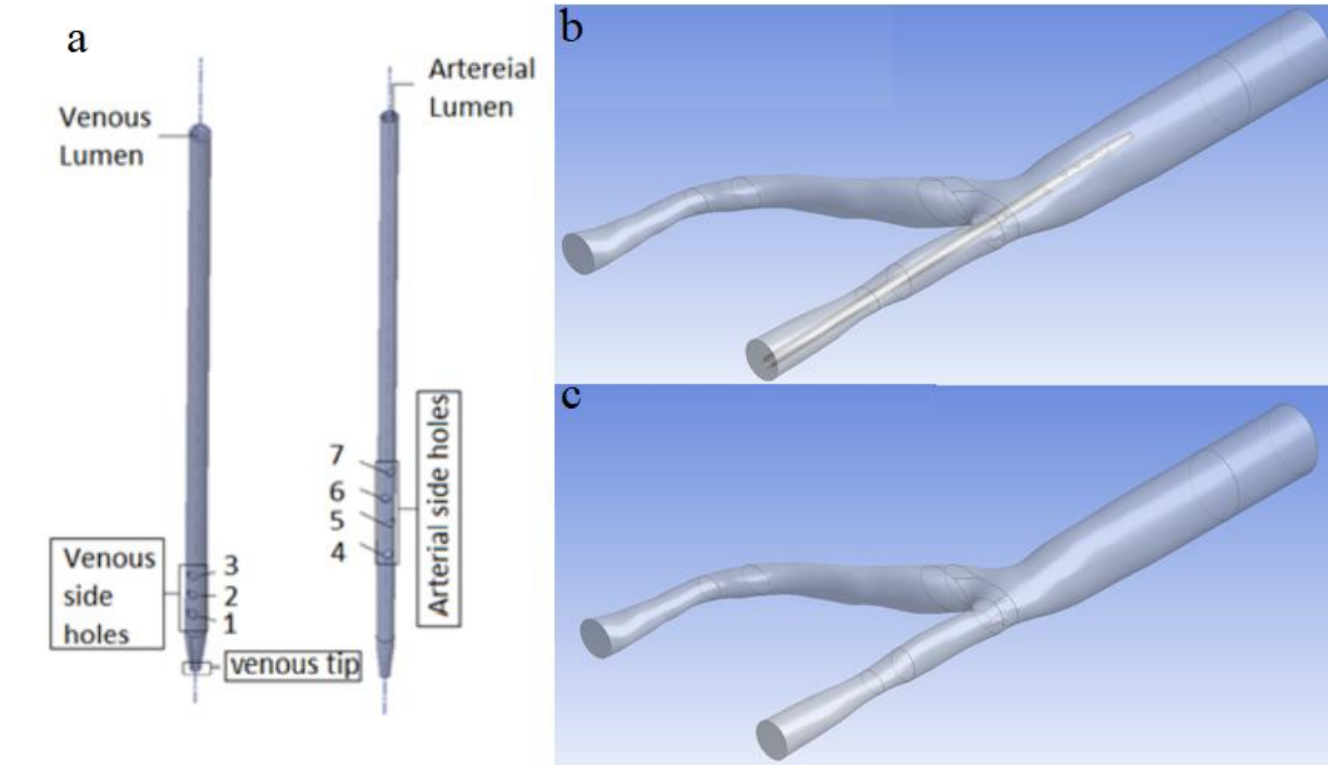

Figure 2. Geometric models developed. (a) Central venous catheter (b) Central veins with the catheter (c) Central veins without the catheter.

The CVC design was characterized by a dual-lumen system, arranged in a single shaft 2 mm in diameter and 20 cm in length. Figure 2a shows the realistic dual-lumen CVC that contains one outflow lumen with three venous outlet holes (1, 2, 3) and a venous tip. It was also shown, in Figure 1a, the second inflow lumen with four arterial inlet holes (4, 5, 6, 7). The internal cross-sectional areas of both the arterial and venous lumens were 2.93 mm^2 .

2.2 Numerical solution

Numerical simulations were performed in transient regime, covering a total time interval corresponding of two complete cardiac cycles of 0.8 s. To meet the adaptive time step criterion, called the *Courant-Friedrichs-Lewis* Condition *(CFL)*, 800 time steps of 0.002 s were considered. The flow inside the catheter was considered steady, with a total mass flow rate of 0.00525 kg/s, as occurs in the clinical hemodialysis procedure. The pressure and velocity coupling was modeled by Coupled algorithm and the second order Upwind discretization scheme was adopted for convective terms.

Kw SST turbulence model was used to characterize turbulence, given its wide use in problems involving blood flow, and its ability to predict turbulence both in free stream regions and close to the boundary layer (Gonçalves *et al.*, 2020). Although blood flow in the human body is essentially laminar, pathological conditions as well as the presence of artificial devices can induce turbulence due to sudden geometric changes in the flow (Shibeshi, S. S., & Collins., 2020; Galdi, *et al.*, 2008). Vergara *et al.* (2017) state that, even at low Reynolds numbers, the pulsatility of the blood flow can make the flow unstable and initiate the transition process to turbulence. These issues, added to the difficulty of calculating the *Re* number for complex geometries of blood vessels and artificial devices (difficult to define a characteristic length) and the non-Newtonian behavior of blood, can make the estimation of the *Re* number quite complex and an unrepresentative criterion to predict the transition to turbulence in these cases.

2.3 Mesh convergence test

Each mesh tested, for both geometry with and without catheter, was generated from the refinement of the previous one, by doubling the number of elements, which resulted in the grid refinement factor (r_{ii}), close to 1.3, as recommended by the ASME V & V 20 standard (McHale *et al.*, 2009). The Characteristic length (h) was calculated by Eq. (1). Eq. (2) presents the way to calculate the refinement factor (r_{ii}), from the characteristic length h, of each mesh.

$$h = \left[\frac{1}{N}\sum_{i=1}^{N}\Delta V_i\right]^{1/3} \tag{1}$$

Where ΔV_i is the volume of the *i* element, and *N* is the total number of elements.

$$r_{ij} = \frac{h_i}{h_j} \tag{2}$$

Where h_i is the course grid, and h_j the fine grid.

Velocity and pressure values were monitored, along the cardiac cycle, in four planes defined close to the region where the tip and lateral orifices of the catheter were located. The choice of location of these planes is justified by the higher strain rate and velocity gradients present in this region. The meshes were refined until the mean value, in the cardiac cycle, of the grid convergence index (GCI), based on the relative error, was less than 5%. Eq. (3) presents the way to calculate the GCI.

$$GCI_{fine}^{i,i+1} = \frac{Fs.e_a^{i,i+1}}{r_{i,i+1}^p - 1} \tag{3}$$

Where $e_a^{i,i+1}$ is the relative error between meshes *i* and *i+1*, $r_{i,i+1}^p$ is the refinement factor, *p* is the apparent order of the method and *Fs* is the safety factor. *Fs* = 1.25 was adopted (McHale *et al.*, 2009).

To meet the convergence criterion, 3 meshes were generated, both for the geometry with and without catheter. Table 1 presents the mean GCI values, along the cardiac cycle, for pressure and velocity, in the four analyzed planes.

Table 1. Grid convergence index (GCI) calculated.

Geometry with Central Venous Catheter		
Location	GCI for Velocity [%]	GCI for Pressure [%]
Plane 01	4.34	1.69
Plane 02	4.93	2.28
Plane 03	5.52	2.64
Plane 04	4.83	1.52
Geometry without Central Venous Catheter		
Location	GCI for Velocity [%]	GCI for Pressure [%]
Plane 01	3.20	1.39
Plane 02	2.53	1.74
Plane 03	2.35	1.67
Plane 04	3.09	1.24

2.4 Boundary conditions

The boundary conditions used in this work were developed from a literature review of studies. The mean values of the curves by Markl *et al.* (2011) and Mynard and Smolich (2015) were used to estimate the total flow in the superior vena cava. The flows in the right and left jugular veins were considered the same and equal to half of the total flow in the superior vena cava. This simplification is justified by the scarcity of data in the literature, in the absence of consensus regarding the flow rate values in the right and left jugular veins and the possible similarity of the flow values between these two veins (Gonçalves *et al.*, 2019; Gonçalves *et al.*, 2020a; Marr *et al.*, 2018; Lucas *et al.*, 2014)

With the estimation of the pulsate flow in each jugular veins and their respective area, was possible to develop the inlet velocities curves for the right and left jugular veins. As a boundary condition at the outlet of the superior vena cava, the pressure curve in the right atrium was adopted, according to Mynard and Smolich (2015). Figure 3 shows the curves developed as boundary conditions in this study.

In Figure 3 the (A) wave occurs when the atrium contracts, increasing atrial pressure. At the same time, the blood is propelled in a retrograde direction toward the veins. When the tricuspid valve closes, the systole wave (S) occurs. The transitional (V) wave corresponds to atrial overfilling against a closed tricuspid valve, anticipating the opening of the valve in diastole (D). The inlet and outlet waveforms designed for this study showed a correlation between flow velocity in the internal jugular veins and the pressure in the right atrium.

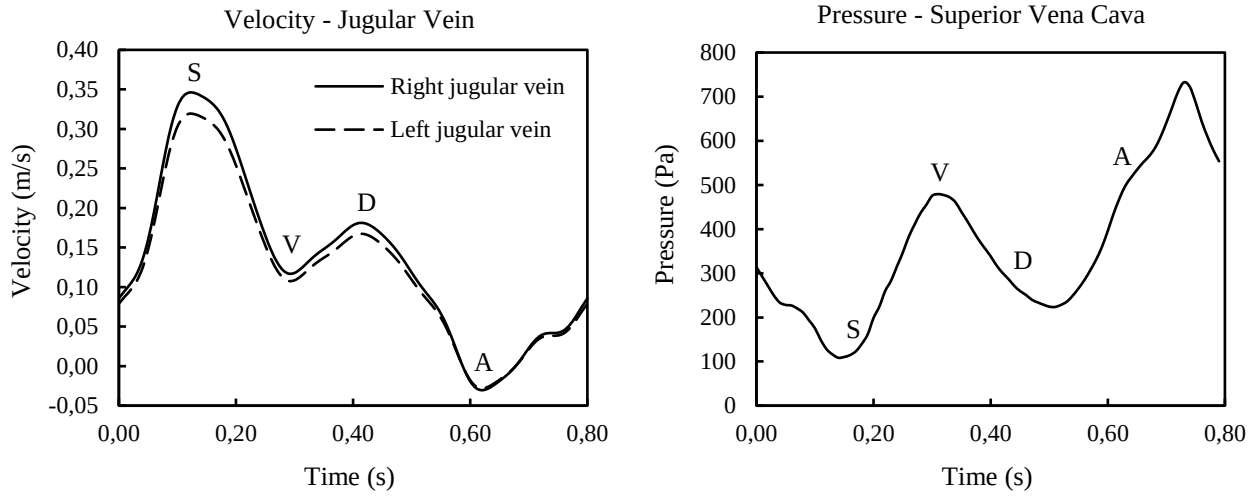

Figure 3. Velocity inlets and pressure outlet curves used as boundary conditions representing the cardiac cycle.

2.5 Fluid rheology

Blood was modeled both as Newtonian and non-Newtonian fluid. When modeled as a Newtonian fluid it was considered a constant viscosity of 0.0035 kg/s (Lucas *et al.*, 2014; Kumar *et al.*, 2019). The density value of 1060 kg/m^3 was considered in booth simulations (Lucas *et al.*, 2014)

The Carreau-Yasuda model is wide used for numerical simulations that need an analytical expression for the blood non-Newtonian viscosity curve (Costa, M.C.B., 2020). According to Kumar *et al.*, (2019) it is the Carreau-Yasuda model which better fits the shear rate relationship and the experimental data.

The viscosity for the Carreau-Yasuda model is given by Eq. (4)

$$\mu = \mu_{\infty} + \left(\mu_0 - \mu_{\infty}\right)\left(1 + (\lambda\dot{\gamma})^a\right)^{\frac{n-1}{a}} \tag{4}$$

Where $\dot{\gamma}$ is the shear rate, μ_0 is the viscosity at zero shear rate, μ_{∞} is the constant viscosity for shear rate values above 100 s^{-1}, λ is the relaxation time, and n is the power law index, whose values, according to Lucas *et al.* (2014) and Kumar *et al.* (2019) are presented in Table 2.

Table 2. Carreau-Yasuda properties used to model the rheological behavior of blood (Kumar *et al.*, 2019; Lucas *et al.*, 2014).

Rheological Model	Maximum Viscosity (kg/m.s)	Minimum Viscosity (kg/m.s)	Power Law index	Time Constant (s)
Carreau - Yasuda	0.056	0.0035	0.3568	3.313

3. RESULTS AND DISCUSSION

The modification of the venous flow pattern induced by the presence of the catheter can change the shear stress distribution, the strain rate and the exposure time of blood particles closed to the region where it is installed, leading to a higher thrombogenic potential (Lucas *et al.*, 2014; Gonçalves, 2020). In order to assess the hemodynamic changes imposed by the catheter, the shear stress values, the strain rate, as well as the overall structure of the flow field were analyzed and compared, in the presence and absence of the catheter.

Figure 4 shows the strain rates distributions along the cardiac cycle in horizontal planes, for the simulations with and without catheter. It is important to highlight that planes P.P and P.O.1 to P.O.8 consist of planes that, respectively, are located closed to the tip and lateral side holes of the CVC. The number of the plane "P.O.N" corresponds to the number of the catheter´s side hole, shown in Figure 2a.

It can be observed that, in Figure 4, the strain rates distribution varies considerably along the cardiac cycle in the jugular veins. In the superior vena cava, this variation was less accentuated, and blood behaves, predominantly, as a non-

Newtonian fluid throughout the cardiac cycle, in both domains, since the strain rate remains at values below 100 s^{-1} (Gonçalves *et al.*, 2019).

Both geometry with and without catheter had strain rate values above 100 s^{-1} in large extension of the jugular veins closed to the occurrence of systole (t = 0.14 s), which suggests that the blood behaves as a Newtonian fluid near this instant of time. The difference in the general distribution of strain rates, as well as in the overall structure of the blood flow field, between the geometry with and without a catheter, was more noticeable at the lower velocity instants of the cardiac cycle, close to diastole. It is noteworthy that significant changes in strain rate and shear stress values along the cardiac cycle can result in a greater process of platelet aggregation and adhesion (Lucas *et al.*, 2014). It was noticed that the catheter significantly increases strain rates as much as the overall pattern of the flow field in the superior part of the vena cava, local where the catheter side holes are located.

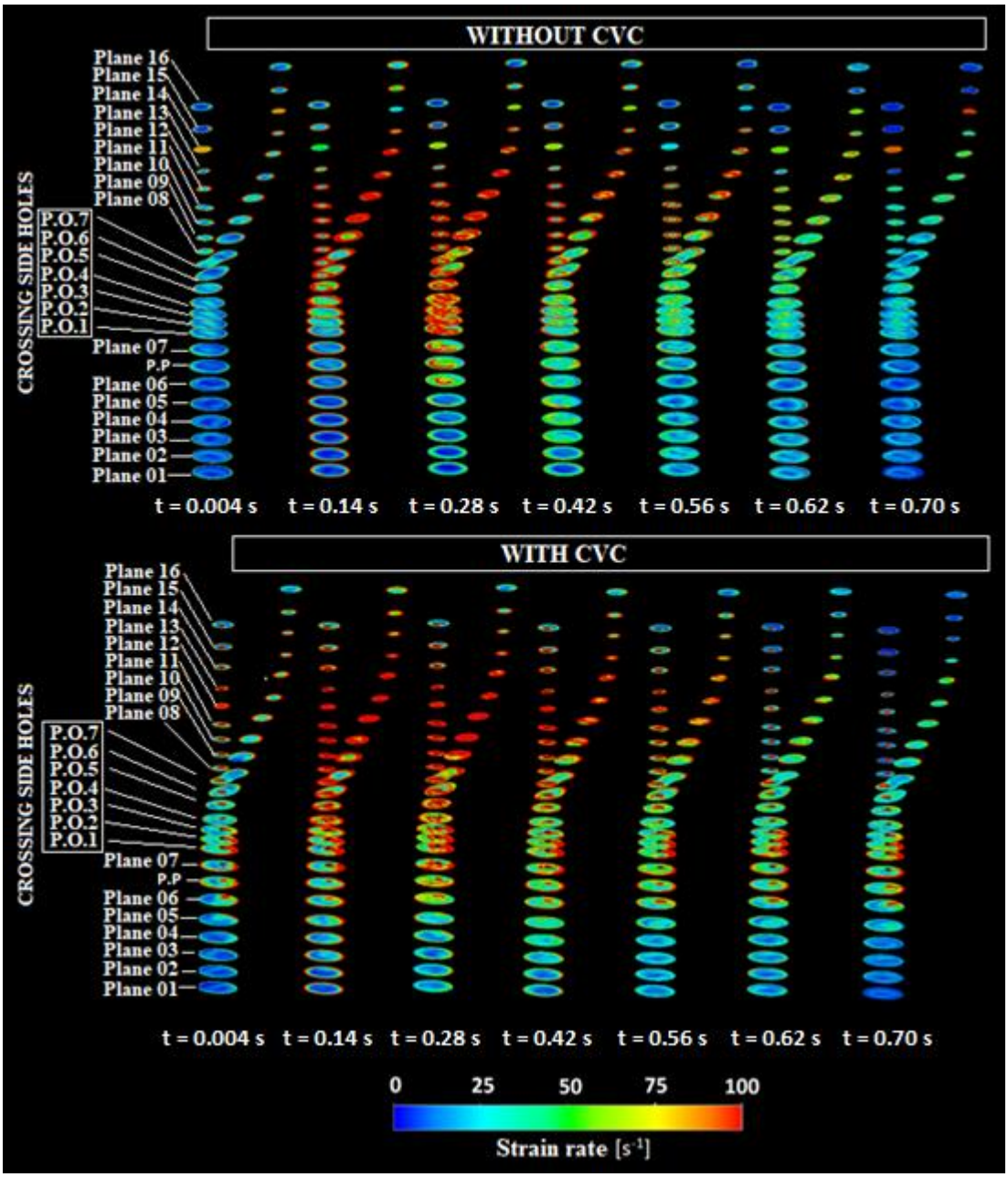

Figure 4. Strain rate distribution along the cardiac cycle.

In order to evaluate and compare the variation of the strain rates along the cardiac cycle, for booth geometries with and without catheter, the mean value of strain rates in different planes of Figure 4 was plotted over in time, as shown in Figure 5.

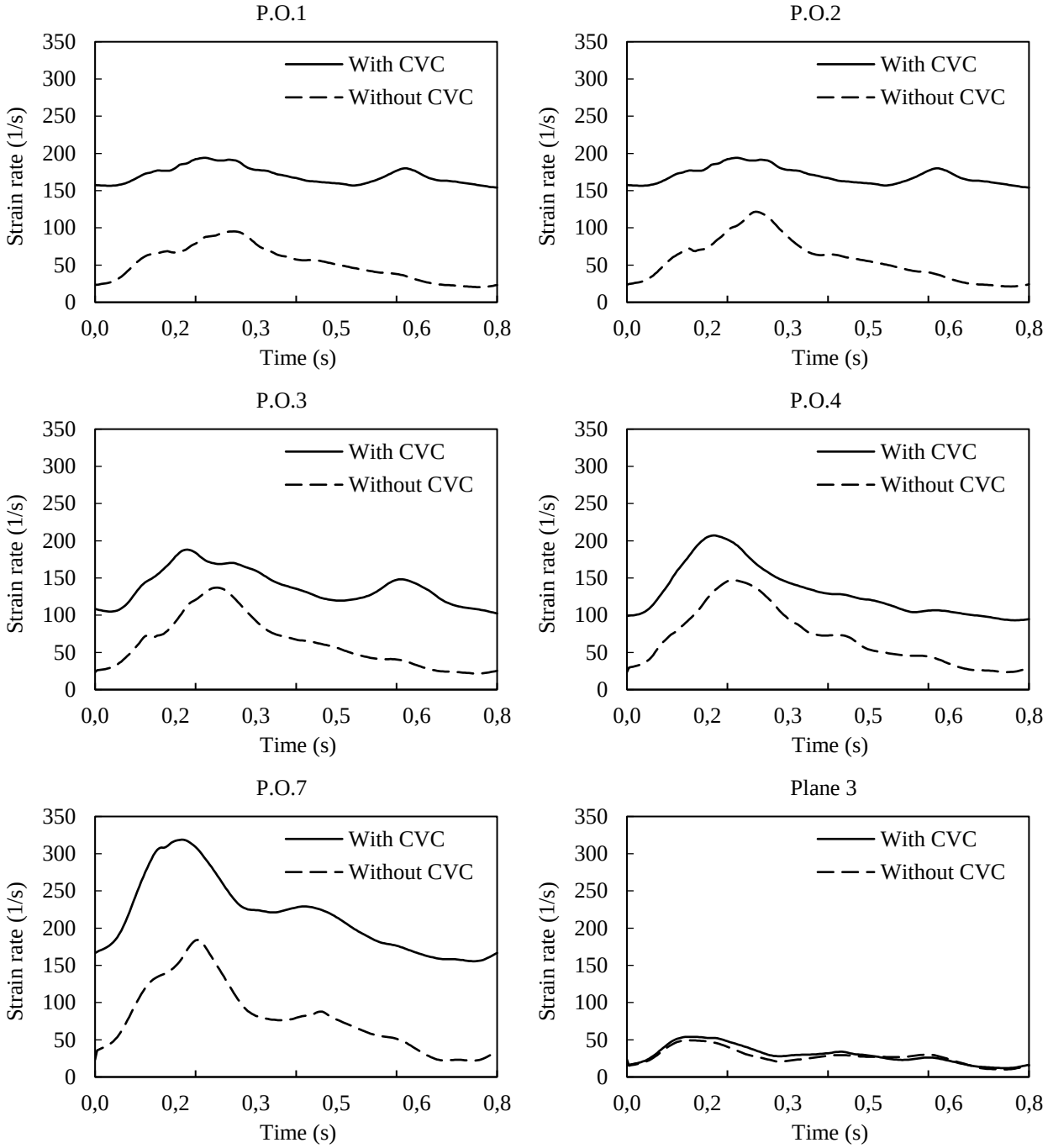

Figure 5. Strain rates along the cardiac cycle in different planes, with and without catheter.

Figure 5 shows that strain rates had considerably higher values in Plane 07. It is noteworthy that the highest shear stress values occurred in the catheter wall, close to orifice 07, as verified by studies in the literature (Lucas *et al.*, 2014; Gonçalves, 2020). In general, the greatest differences in strain rate values between the geometry with and without catheter occur near the instant of time when the flow in the superior vena cava becomes null, just before the reverse flow of the cardiac cycle occurs (t = 0.588 s).

It is observed, in Figure 5, that in all the evaluated planes, except in Plane 03 (the only plane that does not cross the catheter), blood behaves predominantly as a non-Newtonian fluid throughout the cardiac cycle (strain rates lower than 100 s^{-1}), when in the absence of a catheter. In the presence of the catheter, blood behaves, predominantly, as a Newtonian fluid throughout the cardiac cycle. Thus, one of the changes imposed by the catheter in the flow field concerns the change in rheological behavior of blood. This change in the pattern of rheological behavior amortizes the changes imposed on the shear stress field, as blood presents its minimum viscosity value when strain rates assume values greater than 100 s^{-1}, remaining constant for higher values of strain rate (Silveira, 2017; Gonçalves *et al.*, 2019).

In order to evaluate and compare the variation of shear stresses over time, for geometries with and without catheter, the average values of shear stresses in different horizontal planes (showed in Figure 4) were plotted along the cardiac cycle as presented in Figure 6.

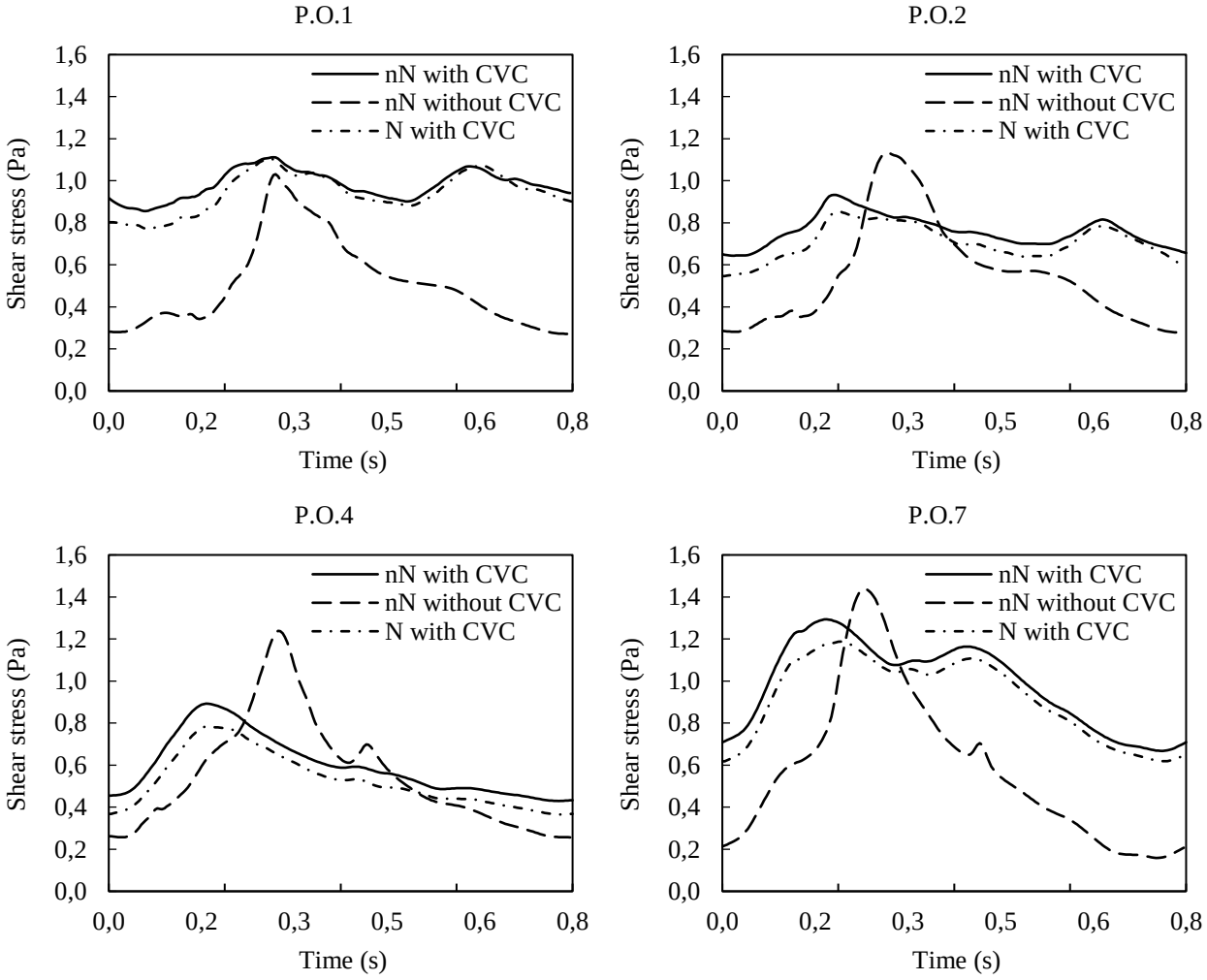

Figure 6. Shear stress in horizontal planes along the cardiac cycle. Where nN: non-Newtonian; N: Newtonian.

Figure 6 shows that changes in shear stress generated by the CVC were most significant moments after diastole, near the beginning and end of the cardiac cycle. Close to systole (t = 0.14 s), these changes were less significant. On the other hand, shear stresses without the catheter were higher close to the time which the pressure in the right atrium grows until it is overfilled against the tricuspid valve, before it opens (t = 0.3 s). At this instant of time, shear stress in the geometry without the catheter surpassed the shear stress in the catheter geometry in several evaluated planes.

Table 3 presents the average values in the cardiac cycle of the shear stress for different planes evaluated in Figure 6. Table 4 presents the comparison between the maximum exposure times on the outflow streamlines of the catheter, at different instants of time along the cardiac cycle.

It can be seen, from the results presented in Table 2 and Table 3, that the variation in shear stress induced by the catheter was percentage less significant and expressive than the variation in the residence time.

These findings reinforce the hypothesis that changes generated by the catheter in the overall structure of the flow field (recirculation, flow separation) are more significant, in thrombogenic terms, than changes in shear stress values. It is noteworthy that regions of recirculation and separation of the flow field tend to increase the exposure time of blood particles and are related to regions of lower shear stress (Berg *et al.,* 2018; Gonçalves *et al.,* 2019).

Table 3. Average shear stress, in the cardiac cycle, for different horizontal planes.

Average shear stress, in the cardiac cycle (Pa)			
Local	With CVC non-Newtonian	Without CVC non-Newtonian	Difference (%)
P.O.1	0.980	0.507	93.294%
P.O.2	0.761	0.549	38.620%
P.O.4	0.597	0.550	8.545%
P.O.7	0.983	0.580	69.469%

Table 4. Residence time on streamlines.

Maximum exposure time on streamlines (s)			
	Without CVC	With CVC	Difference (%)
t = 0.140	0.6277	1.9305	208%
t = 0.400	1.3836	3.4590	150%
t = 0.500	1.4275	10.8445	660%
t = 0.580	43.9677	384.4340	774%
t = 0.620	11.3105	5.2070	-54%
t = 0.800	2.9043	2.0410	-30%

It is also observed, in Figure 6, that the consideration of blood as a Newtonian fluid resulted in lower shear stress values than the use of the non-Newtonian model. This result is expected, once blood non-Newtonian viscosity assumes its minimum value for strain rates greater than 100 s^{-1}, a value from which blood behaves as a Newtonian fluid, with constant viscosity (Silveira, 2017; Gonçalves *et al.*, 2019). The fact that blood viscosity decreases with increasing strain rates has a physiological functionality. In that way, the effect of partial obstructions on the blood flow field tends to be minimized due to the decrease in viscosity, resulting in smaller shear stress and blood cell damage. (Pereira *et al*., 2019).

4. CONCLUSIONS

When comparing the hemodynamic environment in the central veins with and without catheter, it can be seen that the catheter is responsible for raising the values of strain rate, shear stress, as well as generating regions of recirculation, stagnation, and separation of the flow field. The comparison of the percentage increase in shear stress values, in horizontal planes throughout the simulation domain, and maximum exposure time along the flow streamlines, with and without catheter, reinforce the hypothesis that the increase in maximum exposure time (due to recirculation and disturbances generated by the catheter in the flow field) is more significant for thrombus formation in the region than the increase in shear stress.

In general, the greatest differences in strain rate values between the flow with and without the catheter occurred close to the time when the flow in the superior vena cava becomes null (just before the reverse flow of the cardiac cycle occurs, t = 0.588 s). This instant of time results in the longest maximum exposure times in the flow streamlines originated in the venous lumen of the catheter, as well as in larger regions of recirculation and disturbances in the flow field. This finding suggests that the increased flow strain rates are mainly associated with recirculation regions and disturbances in the flow field generated by the catheter.

5. REFERENCES

Berg N, Fuchs L, Prahl L (2018). “Flow Characteristics and Coherent Structures in a Centrifugal Blood Pump”. *Flow,TurbulenceandCombustion*.

Bream (2016). “Update on Insertion and Complications of Central Venous Catheters for Hemodialysis”. *Seminars in Interventional Radiology*, Vol. 33, No. 1, pp. 31–38.

Costa, M.C.B.,2020. Avaliação numérica de diferentes modelos matemáticos para a quantificação de potenciais hemolítico e trombogênico no acesso venoso central para a hemodiálise. Universidade Federal de Minas Gerais, Belo Horizonte, Brasil.

Galdi, et al., (2008). *Hemodynamical flows*. Delhi Book Store.

Chan *et al*., (2019). " Dialysis initiation, modality choice, access, and prescription: conclusions from a Kidney Disease: Improving Global Outcomes (KDIGO) Controversies Conference". *Kidney International*, Vol. 96, No. 1, pp. 37–47.

Gonçalves *et al.,* (2019). "Comparison of different rheological models for computational simulation of blood flow in central venous acess" In *Proceedings of the 22nd International Congress of Mechanical Engineering - COBEM 2019*.

Gonçalves,S.F.,2020. Avaliação numérica do efeito da variação da vazão na hemodinâmica em cateter venoso central para a hemodiálise". Masters dissertation, Universidade Federal de Minas Gerais, Belo Horizonte, Brasil.

Gonçalves, S. D. F. et al., 2020a. Evaluation of Different Turbulence Models for the Characterization of Shear Stresses in the Central Venous Access for Hemodialysis. *In Proceeding of the 18nd Brazilian Congress of Thermal Sciences and Engineering*. November 16-20, 2020.

Kumar *et al.,* (2019). "Computational fluid dynamic study on effect of Carreau: Yasuda and Newtonian blood viscosity models on hemodynamic parameters". *Journal of Computational Methods in Sciences and Engineering,* pp.1-13.

Lucas *et al.,* (2014) "Blood Flow in Hemodialysis Catheters: A Numerical Simulation and Microscopic Analysis of In Vivo-Formed Fibrin". *Artificial Organs*, Vol. 38, N° 7, pp. 556–565

Male *et al.* (2015). "Central venous catheter-related thrombosis and thromboprophylaxis in children: A systematic review and meta-analysis: Discussion". *Journal of Thrombosis and Haemostasis,* Vol. 13, No. 4, pp. 688–690.

Markl, M. et al., 2011. Time-resolved three-dimensional magnetic resonance
velocity mapping of cardiovascular flow paths in volunteers and patients with Fontan circulation. *European Journal of Cardio-thoracic Surgery*, Vol. 39, No. 2, pp. 206–212.

Marr, K. et al., 2018. Jugular Venous Flow Quantification Using Doppler Sonography. Ultrasound in Medicine and Biology, Vol. 44, No. 8, pp. 1762–1769

McHale, M. P., Friedman, J. R., & Karian, J. (2009). Standard for verification and validation in computational fluid dynamics and heat transfer. *The American Society of Mechanical Engineers*, ASME V&V, 20.

Mynard, J. O. P. M. and SMOLICH, J. O. J. S. One-Dimensional Haemodynamic Modeling and Wave Dynamics in the Entire Adult Circulation. *Annals of Biomedical Engineering*, Vol. 43, No. 6, pp. 1443– 1460

Neves *et al*., (2020). "Analysis of data from the 2009-2018 decade". *Brazilian Journal of Nephrology*, pp. 1–10.

Peng *et al.,* (2017). "Numerical Simulation of Hemodynamic Changes in Central Veins after Tunneled Cuffed Central Venous Catheter Placement in Patients under Hemodialysis". *Scientific Reports*, Vol.7, No 1, pp. 3–10.

Pereira, M. G.; Finzer, J. R. D.; Mamagoni, R. A.,2019 "Rheological evaluation of blood flow". *Brazilian Journal of Development*, Vol. 5, pp. 3042–3050.

Shibeshi, S. S., & Collins, W. E. (2005). The rheology of blood flow in a branched arterial system. *Applied Rheology*, 15(6), 398-405. https://doi.org/10.1515/arh-2005-0020

Silveira, M., 2017. "Simulação numérica de escoamento pulsátil na aorta torácica e aneurisma". Masters dissertation, Universidade Federal de Minas Gerais, Belo Horizonte, Brasil.

Vergara *et al.,* (2017). Large eddy simulations of blood dynamics in abdominal aortic aneurysms. *Medical engineering & physics*, Vol. 47, pp. 38-46.

6. RESPONSIBILITY NOTICE

The author(s) is (are) the only responsible for the printed material included in this paper.

The geometry of internal jugulars vein and superior vena cava used in this study was obtained from handling computed tomography (CT) images of a male healthy patient of 74 years old. The procedure was approved by the "Comitê de Ética em Pesquisa/Universidade Federal de Minas Gerais (CEP-UFMG) under process number CAAE 02405712.5.1001.5149".